Butler-based thermodynamic modelling of interfacial energies for in-vessel corium systems

Kasi Gajavalli, Romain Le Tellier

Butler-based thermodynamic modelling of interfacial energies for in-vessel corium systems

Kasi GAJAVALLI, Romain LE TELLIER[1]

CEA, DES, IRESNE, DTN, Saint Paul-lez-Durance, Cadarache, F-13108, France

Abstract

The modelling of transient phase segregation phenomena in corium multicomponent thermodynamic systems is limited especially in the liquid miscibility gap which can lead to phase separation (stratification of the liquid phases for corium) and is of tremendous importance. The modelling of the associated phase separation transients in corium stratification is limited by a deficiency in the interfacial energy data, which are difficult to measure experimentally for these high-temperature systems. The limitations of summarizing the interfacial energies as constant coefficients were observed in a recent work on simulation of the stratification kinetics of a corium pool and the necessity to improve the estimation of interfacial energies [1], [2]. This work tests the efficacy of a thermodynamic approach to evaluate the interfacial tensions, initially proposed for metallic systems by Kaptay [3]. This method is based on the Butler equation and makes use of existing thermodynamic databases for multicomponent systems constructed by the CALPHAD method. In practice, the application of this method to corium systems was performed using the open-source code openIEC [4]. To do so, this code was modified to enable required features, both functionally and methodically. In particular, the OpenCalphad Gibbs energy minimizer has been interfaced in this framework and benchmarked against previous results was carried out. Then, interfacial energies were calculated for two relevant corium systems (U-O and U-O-Zr-Fe) using two different existing databases (TAF-ID and NUCLEA). The first

[1] Corresponding author: romain.le-tellier@cea.fr

results obtained were analyzed in terms of general trends and compared to existing theoretical aspects. Large differences were observed depending on the thermodynamic database that was used.

1 INTRODUCTION

In a severe accident scenario leading to core degradation, a pool of molten chemical mixtures comprising of the fuel and structural elements of the core which is commonly called ‘corium' is formed and might relocate to the lower plenum of the Reactor Pressure Vessel (RPV)[5]. This corium pool exhibits a liquid phase separation known as stratification between two immiscible liquids, one of metallic character and the other oxidic. The nature of the immiscible liquid phase separation is decisive with respect to the distribution of the heat flux at the vessel lower head boundary and is driven by chemical and convective mass fluxes.

The simulation of transient in-vessel corium stratification involves multicomponent and multiphasic transport models. One such model is based on an approach coupling the Cahn-Hillard equation (describing component mass transport) to the Navier stokes equation (describing laws of fluid flow), which require data relating to interfacial energies [2], [6]–[8]. For modelling purposes, the segregation models rely on the detailed representation given by specific thermodynamic databases (obtained by the CALPHAD method [9]) for the description of the homogeneous phases, but the closures associated with these interfacial energies is, in practice, restricted to constant parameters that are adjusted on a “case-by-case” basis. Some recent works related to the simulation of the stratification kinetics of a corium pool have clearly highlighted the limits of such an approach and the necessity to go further and acquire composition-dependent data for these interfacial energies [1].

Note that similar deficiencies in the interfacial energy data holds true when considering the modelling of liquid/liquid demixing process in preparation of molybdenum oxide concentrates (nuclear waste vitrification process) which lead to the formation of separate molybdenum oxide enriched phases and their coalescence. These processes modify the rheological and electrical properties of liquids at high

temperature and the homogeneity of the glass after cooling [10]. The liquid-liquid energy and density difference play a crucial role in the demixing process. This work focusses on corium systems which is a part of long-term project where both, the corium and nuclear glasses materials are considered.

The measurement of surface tension between a condensed phase (liquid) and a gaseous phase has been the subject of numerous investigations, resulting in an array of techniques whose theoretical foundations and experimental issues are widely documented. The implementation of several of these techniques on the VITI installation (maximum bubble pressure, sessile drop) of the PLINIUS platform [11], [12] at CEA Cadarache and on ATTILHA (aerodynamic levitation, acoustic oscillator) [13] at CEA Saclay enabled these years of obtaining original results for steels, corium or even corium / concrete mixtures. However, the interfacial tension between two condensed phases (liquid/liquid system) are much rarer.

From an experimental point of view, the metallic-oxidic systems are difficult to investigate at very high temperatures (>2800 K) due to crucible compatibility issues, contamination by surface-active impurities, increased heat transfer, establishment of the physico-chemical equilibrium, evaporation, diffusion, etc. and most of these problems scale with experimental duration and usually lead to a large errors. To the best of our knowledge, there are no measurement data on the interfacial energies available for the corium systems. As a result, the associated closures in segregation models are limited to the use of constant values evaluated a priori for a given composition of the phases present by means of Girifalco-Good type correlations, which permits interfacial energy to be evaluated from surface tensions [14].

State-of-the-art thermodynamic description of the condensed phases associated with corium is given by CALPHAD databases and this paper makes an attempt to use this capitalized knowledge to evaluate interfacial energies by a thermodynamic model. At this stage, it should be noted that such databases were not developed with calculating interfacial energies in mind and that these databases capture behaviors at moderate temperatures fairly well but have greater uncertainties at high temperatures due to limited experimental data, in particular calorimetry measurements. For instance, considering the U-

O liquid model, the assessment mainly relies on measurements of a single tie-line and heat capacity data for pure U or pure UO_2. Accordingly, this works should be seen as a "proof-of-principle" for evaluating interfacial energies for corium systems using CALPHAD databases.

In the current study, the thermodynamic approach based on the Butler equation [15] is studied to evaluate the interfacial energies and will be discussed in the subsequent section. The discussion will be followed by the available implementation of the procedure through the openIEC code [4] modified to fulfil the requirements of the current study. The code will be tested for specific compositions of the liquids present in the U-O binary system and extended to the U-O-Fe-Zr quaternary system. A comparison of the results thus obtained will be done with the previous literature methods [3], [4], [14]. In addition, a parametric study will be carried out to better understand the model parameters sensitivity to the database employed through comparison of results when using NUCLEA [16], [17] and TAF-ID databases [18].

2 THERMODYNAMIC MODELLING: THE RENOVATED BUTLER EQUATION

The Butler equation is generally used to calculate the surface segregation, surface adsorption and surface tension of liquid solutions. In due course, the equation was extended to calculate the interfacial composition and interfacial energies for solid/liquid interface, coherent interfaces and even grain boundaries.

The historical derivation of the Butler equation is cumbersome (introducing ill-defined partial surface tensions) and based on a mono-layer hypothesis that can appear as a strong limitation. However, in the recent developments, it was renovated and extended by Kaptay [3] to liquid/liquid and liquid/solid interfaces. In particular, in the case of a coherent interface, the scope of application of this renovated Butler equation appears as very general.

Let us consider a system with N components and two phases (α and β) of molar composition denoted respectively by $\{n_i^\alpha\}_{1\leq i\leq N}$ and $\left\{n_i^\beta\right\}_{1\leq i\leq N}$ at thermodynamic equilibrium separated by an interface ζ. If G denotes the Gibbs energy of the system, the interfacial energy is [19], [20],

$$\sigma = \left(\frac{dG}{dA}\right)_{p,T,n_i} \quad (Eq.\,1)$$

where p is pressure, T is the absolute temperature and A is the interface area. The interface is of unspecified thickness and structure but it is considered that it can be treated as a phase and can be fully described by its overall composition denoted $\left\{n_i^\zeta\right\}_{1\leq i\leq N}$. Under these conditions, in addition to the classical condition of chemical potentials equality between α and β phases for any component ($\forall i$, $\mu_i^\beta = \mu_i^\alpha \equiv \mu_{i,eq}$) [19], the equilibrium conditions result in: $\forall i$,

$$\sigma = \frac{\left(\mu_i^{*,\zeta} - \mu_i^\alpha\right) + \left(\mu_i^{*,\zeta} - \mu_i^\beta\right)}{\omega_i} \quad (Eq.\,2)$$

where:

$\omega_i = \left(\frac{\partial A}{\partial n_i^\zeta}\right)_{T,p,n_{j\neq i}^\zeta}$ ($m^2.mol^{-1}$) is the partial molar surface associated with the component 'i';

$\mu_i^\alpha = \left(\frac{\partial G^\alpha}{\partial n_i^\alpha}\right)_{T,p,n_{j\neq i}^\alpha}$ and μ_i^β ($J.mol^{-1}$) are the chemical potentials of both phases for component 'i';

$\mu_i^{*,\zeta} = \left(\frac{\partial G^\zeta}{\partial n_i^\zeta}\right)_{T,p,n_{j\neq i}^\zeta}$ ($J.mol^{-1}$) is the reduced chemical potential of the interface associated with component 'i'. As in [3], "reduced" is used to refer to $\mu_i^{*,\zeta}$ because the actual partial Gibbs energy of the system w.r.t. n_i^ζ is composed of two terms $\mu_i^{*,\zeta}$ and $\sigma\omega_i$. Exponent * is used to highlight it.

Eq. 2 can be simplified as, $\forall i$,

$$\sigma = 2\frac{\Delta\mu_i}{\omega_i} (\equiv \sigma_i) \quad (Eq.\,3)$$

where the term $\Delta\mu_i = \left(\mu_i^{*,\zeta} - \mu_{i,eq}\right)$ is the chemical potential (partial Gibbs energy) change by a transfer of 1 mol of component *'i'* from the bulk phases to the interfacial layer (ζ) and ω_i ($m^2.mol^{-1}$) is the partial molar surface of component *'i'*.

For the liquid/liquid interface (consistent interface), the interfacial energy is calculated from only the bulk Gibbs energy (i.e., $G^\zeta = G^\alpha = G^\beta$) and the partial molar surfaces of the components (ω_i). The partial molar surfaces can be related to the partial molar volumes [21] in an approximate way described in the extension of the formalism of the Butler equation [3] by

$$\omega_i = f.V_i^{2/3}.N_{Av}^{1/3} \quad (Eq.4)$$

where f is a factor that depends on the packing fractions of the bulk phase and interface ($f \cong 0.806$) [3], while N_{Av} is the Avogadro number ($N_{Av} \cong 6.023 \times 10^{23}\ mol^{-1}$). and V_i is the partial molar volume of component *'i'*.

The interfacial layer will be in equilibrium if the partial interfacial energies σ_i (see Eq. 3) of all components equal each other. Henceforth, for a '*N*'-ary system, (*N*-1) equations are to be solved to look for the interfacial composition (in terms of molar fraction $\{x_{j,\zeta}\}_{1\leq j\leq N-1}$), such that $\forall i \in [\![1, N-1]\!],\ \sigma_i = \sigma_N$. The above method presents a simpler thermodynamic approach without complex parameters such as thickness of the interfacial layer, the gradient energy coefficient, the concentration gradient across the interface, the structure of the bulk phases and the ratio of the broken bonds.

At critical temperatures, the approximated equality of partial interfacial energies holds and the interfacial energy tends to 'zero' as the different phases dissolve into a single phase and the interface between them disappears. The equation was tested on binary and ternary metallic phases with coherent interfaces and the results obtained showed a consistent trend with respect to temperature [3].

2.1 NUMERICAL APPROACH AND IMPLEMENTATION

Different approaches can be adopted to numerically solve the non-linear system associated with the Butler equation. For corium, this methodology has to be extended to deal with more complex

representation of Gibbs energy of the liquid phase, in this case, associated model and ionic model for which the number of constituents (defining the variables of the function) is greater than the number of system components.

One method is the *constrained Gibbs energy minimization* technique where the interfacial energy can be recast as a minimization problem and can be solved using Gibbs energy minimizer tools such as OpenCalphad (OC) [22], [23] with appropriate modifications to the database (in particular, introducing a specific phase for the interface and virtual components). However, in the present work, this approach has not been pursued as it requires modifications in the database itself to introduce data associated with the interface phase.

Another method is the direct solution of Eq. 3, *i.e.* the interfacial composition is searched in such a way to satisfy the equilibrium conditions over the interface and subsequently deduce the interfacial energy of the components. This approach was implemented in openIEC [4], an open-source code based on the pyCalphad [24] Gibbs energy minimization package and Calphad database manipulation. The openIEC code evaluates the temperature and composition dependent interfacial energies of alloys with an arbitrary number of components for solid/liquid and coherent interfaces using Kaptay's methodology.

For evaluating the interfacial energy of a complex thermochemical system such as U-O-Zr-Fe and also for better integration purposes with the tools developed at CEA, OpenCalphad was used to modify openIEC (based on pyCalphad). This modification is mandatory in order to treat the interfacial energy in a miscibility gap. Indeed, "local" minimization (*i.e.* minimization of the Gibbs energy of a single phase

in terms of constituent fractions for a given element inventory)[2] without considering phase separation in a miscibility gap is not supported yet by pyCalphad (it is in development stage [24]) and is required for computing $\left\{\mu_i^{*,\zeta}\right\}_{1\le i\le N}$ for a given interface composition $\left\{x_{j,\zeta}\right\}_{1\le j\le N-1}$ when solving the Butler equation for an interface of two phases in equilibrium in a miscibility gap.

Two types of equilibrium calculations have to be distinguished:

1. the calculation of the composition that minimizes the energy of the system with activation of the search for the miscibility gap for which the state obtained corresponds to a liquid phase exhibiting segregation with two different compositions: the minimum energy obtained is the global minimum;
2. the calculation of the constituent composition which minimizes the energy of a single phase without looking for the miscibility gap for a given element inventory. This minimization procedure differs from the previous one since the liquid phase can only have one composition; this is a "local" minimum.

[2] The Gibbs energy model of a phase is, expressed in terms of constituent fractions (possibly over different sublattices). These constituents can be different from the elements. For instance, in NUCLEA, with the non-ideal associate model, the liquid phase for the ternary system U-O-Zr is described in terms of the fractions of U, Zr, O, UO2 and ZrO2 constituents. Accordingly, it is a function of three molar fractions (while the element composition is only defined by two variables). It is the minimization of the phase Gibbs energy function with respect to such extra degrees of freedom that we refer by "local" minimization. In the U-O-Zr case, this minimization can be interpreted in terms of the following redox reaction $U + ZrO_2 \rightarrow UO_2 + Zr$ [54].

It is precisely the second option which that evaluates $\left\{\mu_i^{*,\zeta}\right\}_{1\le i\le N}$ for a given interface composition $\left\{x_{i,\zeta}\right\}_{1\le i\le N-1}$; for metallic/oxide corium systems, it corresponds to the local chemical equilibrium of the oxidation-reduction reactions for given element composition. OC permits global equilibrium calculations detecting automatically miscibility gaps using the so-called grid-minimizer algorithm for phase compositions initialization: in the case of a miscibility gap, two or more different compositions can be distinguished in this way for a same phase. When the grid-minimizer is not used, miscibility gap are not detected and, accordingly, metastable single-phase equilibrium calculation cannot be performed.

With the above observations, the pyCalphad (Python) has been replaced by OpenCalphad (Fortran) in the frame of openIEC.[3] To do so, a python interface for OC was developed using the f90wrap tool [25]. This tool is also used extensively in QUIP (Quantum Mechanics and Interatomic Potentials) [26] and CASTEP DFT [27] code. The python interface for the OC code gives access to the subroutines, derived types and data of OC that are available in the existing Fortran and C++ OCASI interface provided with OC.[4]

Then, in openIEC, molar volumes of the phases forming the interface is computed by giving the molar volume of pure components taken from different molar volume databases [28]. These molar volumes are not a function of composition and only depend on temperature. For corium systems, such a molar volume database is not available and mass density is not a direct function of the component composition so that partial molar volumes may depend on the element composition. Accordingly,

---

[3] This modified version of openIEC is freely available as a fork from the original github repository at https://github.com/niamorelreillet/openiec_with_OC.

[4] This python interface for OC has been integrated into OC available on github at https://github.com/sundmanbo/opencalphad.

another modification carried out in the openIEC code is the methodology used for calculation of the partial molar volumes with respect to component *'i'*. In the present work, the phase molar volumes are obtained from the mass densities of the oxide and metallic phases of the U-O-Zr-Fe quaternary system. These densities are evaluated from an ideal mixing laws using species mass densities compiled from various literature works. Such an approach was applied to the interpretation of the MASCA experiments and was found in fair agreement with the experimental results [29]. Then, partial molar volumes of components are calculated as the first order volume derivative evaluated by a second-order finite difference formula.

More precisely, for a given temperature T, the derivative of volume V at a composition $\{n_j\}_{1\leq j\leq N}$ with respect to n_i is approximated by:

$$V_i = \left(\frac{\partial V}{\partial n_i}\right)_{n_{j\neq i}} = \left(\frac{V(\underline{n}^{i,+}) - V(\underline{n}^{i,-})}{2\varepsilon}\right) \qquad (Eq.5)$$

where $V(\underline{n}^{i,\pm})$ is the volume evaluated for composition $\underline{n}^{i,\pm} = \{n_1, \dots n_i \pm \varepsilon, \dots n_N\}$. Once the partial molar volumes for all the elements are obtained, an approximated volume is computed by

$$V_{approx} = \sum_{i=1}^{N} n_i V_i \qquad (Eq.6)$$

and a control on the associated accuracy is performed to ensure that the choice of ε is correct. This volume is calculated by $V = \frac{m}{\rho}$ where m is the mass associated with $\{n_j\}_{1\leq j\leq N}$ and ρ is the mixture mass density. While the mass is obtained from OC, the density is determined from the constituent mass fractions (obtained by converting the constituent molar functions) and constituent mass density laws of the endmembers (*i.e.* stoichiometric species) [29].

In order to ensure consistency in the Butler equations solution, the partial molar volume should be evaluated at the interfacial composition. To do so, an iterative procedure has been adopted. For a given initial guess of the interfacial composition $\{x^0_{i,\zeta}\}_{1\leq i\leq N-1}$, the partial molar volumes are evaluated and

the Butler equations solved to get a new approximation of the interfacial composition $\{x_{i,\zeta}\}_{1\leq i\leq N-1}$; $\{x_{j,\zeta}\}_{1\leq j\leq N-1}$ is then compared with $\{x_{i,\zeta}^{0}\}_{1\leq i\leq N-1}$ and the process is iterated until the convergence criteria $\|x_{j,\zeta}^{0} - x_{j,\zeta}\| < 10^{-5}$ is satisfied.

2.2 VERIFICATION

With the above modifications incorporated, the code will be tested for oxide systems for the first time in this work as the modified code can now handle metastable equilibria calculations in the miscibility gap. Before that, different verification exercises were carried out: the modified code was has been used to calculate the interfacial energy for the Ni-Al, Ni-Al-Cr systems against the openIEC original version [4]. As an example of this verification process, the interfacial energy as obtained from both pyCalphad-based and OpenCalphad-based solutions of Eq. 3 is depicted in Figure 1 for a given global composition in the γ/γ' coherent phases region (defined by $x_{Al} = 0.18, x_{Cr} = 0.0081, x_{Ni} = 0.8119$) over the 1250-1450 K temperature range. It can be seen that the difference between both solutions is always lower than 10^{-7} N.m^{-1}.

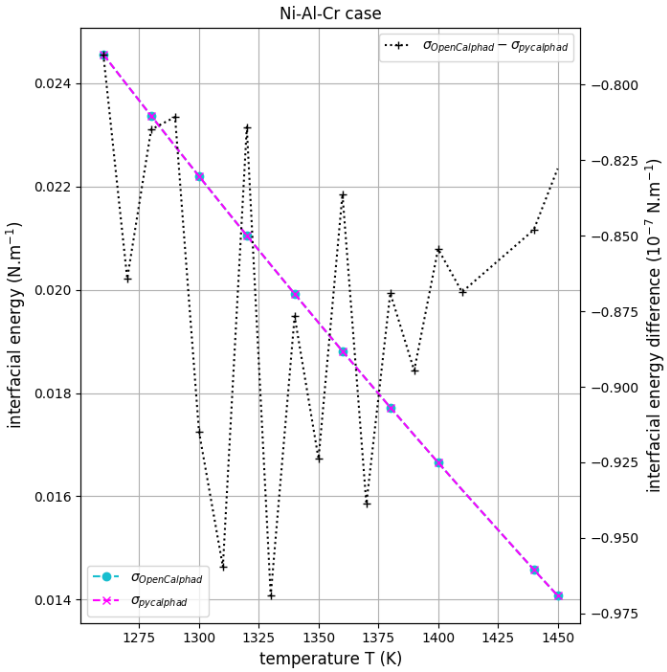

Figure 1: Comparison of interfacial energy of the γ/γ′ coherent phases in the Ni-Al-Cr ternary system calculated with the openIEC code either with pyCalphad (native openIEC implementation) and OpenCalphad (this work).

In any case, these calculations reproduced the pyCalphad results by replacing it with OC. Note that for lower temperatures where a miscibility gap in the γ' phase exists, because of the pyCalphad limitations regarding metastable equilibrium calculation, phase separation was not disabled in OC to make OC results comparable for verification purpose. Accordingly, the results were found consistent between both codes (as expected) but clearly unrealistic. In view of published results with openIEC [4], it can be thought that the authors used a modified version of pyCalphad that enables metastable equilibrium calculation but this information is not mentioned in the article and neither is this feature available in the current pyCalphad version.

3 NUMERICAL RESULTS: APPLICATION TO CORIUM SYSTEMS

NUCLEA [30], [31] and TAF-ID (Thermodynamics of Advanced Fuels-International Database) [32] databases will be used in this work for calculating interfacial energies with openIEC using OC for corium systems. Before elaborating on the results, it is important to highlight the difference in the

representation of thermodynamic data in both the databases. Eventually, the consequences and approach to solve for interfacial energies are discussed.

In NUCLEA, the Gibbs energy of the liquid phase is described using the non-ideal 'associate' model with a single sub-lattice. This takes into account the interactions between the elements to form associate species. These stoichiometric compounds are the constituents of this sub-lattice and also are the endmembers. The Gibbs energy functions are written in terms of species (constituent) compositions and the introduction of 'associate species' as a new constituent for writing the Gibbs energy of formation, which provides an internal degree of freedom that can be used to better capture experimental data. At very high temperatures, the composition and temperature dependence of Gibbs energy of the metallic phases are most of the times estimated/extrapolated [33], [34]; it is well established that the choice of the model can have great impact on the shape of the miscibility gaps in demixing systems [35][29].

On the other hand, the TAF-ID database uses the ionic two sub-lattice model to describe the liquid phase. In this model, one sub-lattice is composed of constituents in the form of cations 'A', and the other sub-lattice consists of anions 'B'. The compounds with a specific constituent on each sublattice are used to create the Gibbs energy expression. Here, the compound is the endmember of the phase, which the phase can exist with only a single endmember and the fractions of different endmembers vary when the composition varies. Hypothetical vacancies 'VA' and neutral species are introduced in the second sub-lattice to model metallic liquid and non-metallic liquid systems respectively. For instance, for the U-O system, the two-sublattice model can be summarized as $(U^{4+})_P(O^{2-}, Va^{Q-}, O)_Q$. The vacancy can be a constituent of any sub-lattice and thus contribute to the configurational entropy while it automatically cancels out in the evaluation of other terms (like surface of reference, excess Gibbs energies) that contribute to the total Gibbs energy.

In both the databases, the considered experimental data at high temperature (the interest of this study) is very scarce. Especially, in the region of the liquid miscibility gap, experimental data is extremely hard to measure due to technological limitations and scientific complications that arise for these elements

at high temperature. Therefore, one has to keep in mind that the databases used in this study come with a large uncertainty on the thermodynamic description of the liquid phase of interest. In other words, knowingly, this "proof-of-principle" work makes use of these databases out of their strict range of application.

In subsequent sections, interfacial energy is evaluated using the openIEC code with the incorporated OC software for the U-O and U-O-Zr-Fe systems in a progressive manner. With the above subtle points and pre-requisite modifications, evaluations are made using both the NUCLEA and TAF-ID databases to highlight the impact (and differences) of the thermodynamic data and also discuss the scope for improvement on various fronts.

3.1 U-O BINARY SYSTEM

The U-O system is an important preliminary step to understand the stratification process in the later stages of fuel degradation. A large experimental and simulation dataset is available for the U-O system at solid state, considering its importance in severe accident analyses [36]–[39]. With these data, thermodynamic databases have been vastly improved and very accurate descriptions have been obtained for the UO_3,U_3O_8, U_4O_9 stoichiometric compounds and the ($UO_{2\pm x}$) solid solution [40]. The thermodynamic models used in this study are leveraged from TAF-ID version 10 [18], [32] and NUCLEA version 19.1 databases. As stated before, at liquid state, experimental data are scarce.

In this section, interfacial energies for the liquid/liquid phase in the U-O phase diagram as evaluated by the modified version of openIEC in the temperature range 2800-4400 K using both NUCLEA and TAF-ID databases.[5] It should be noted that this analysis was conducted on such a large temperature

[5] At a given temperature, only one tie line exists in the miscibility gap region of a binary system. Accordingly, the interfacial energy as calculated with Eq. 2 under equilibrium condition only depends on temperature (and not composition) for such a binary system.

range, in order to study the model behavior and check its consistency. Obviously, only the results below the temperature at which a gas phase is predicted by the global system equilibrium calculation are physically meaningful (with NUCLEA, the gas phase is predicted for temperature higher than 3720K at 1bar and x_U =0.65)

The partial molar volumes of the respective components were calculated following the approach detailed previously. In this approach, the mixture mass density was calculated from the ideal density law of mixture of species and laws of species density as a function of temperature. The species density laws used in analyzing the thermophysical properties of in-vessel corium for the results related to the MASCA program [29] were considered. Knowingly, by considering a temperature range that goes beyond the gas phase appearance, these density laws are used out of their range of validity but, once again, extending the calculations out of the physical range of interest is useful for the sake of model consistency verification as discussed afterwards.

Along with the interfacial energy values, the corresponding equilibrium interfacial composition, molar amounts of the bulk phases and the element composition in the equilibrium phases are also computed in the aforementioned temperature range.

3.1.1 Comparison between NUCLEA and TAF-ID

In Figure 2, the calculated interfacial energies ($\sigma_{calc.NUCLEA}$, $\sigma_{calc.TAF-ID}$) values are plotted against temperature along with a fit according to a 'power law' (used for describing the experimental dependence of the liquid/liquid interfacial tension for monotectic alloys [41]) as follows:

$$\sigma_{fit} = \sigma_0 \left(1 - \frac{T}{T_C}\right)^{\vartheta} \qquad (Eq.7)$$

where, σ_0 is a constant, T is the absolute temperature, T_C is the critical temperature of demixing (consolute point), and ϑ is the critical point exponent. According to the classical theory of van der Waals [42] or the later work of Cahn and Hilliard [43] ϑ is 3/2, while the renormalization group theory of critical behavior gives 1.26 [44]. In this study, we obtain two different values for the interfacial energy

value, $\vartheta_{NUCLEA} = 2.027$ and $\vartheta_{TAF-ID} = 2.155$. Both ϑ values using the NUCLEA and TAF-ID databases are higher than the theoretical value in the literature and significantly different from each other in this regard.

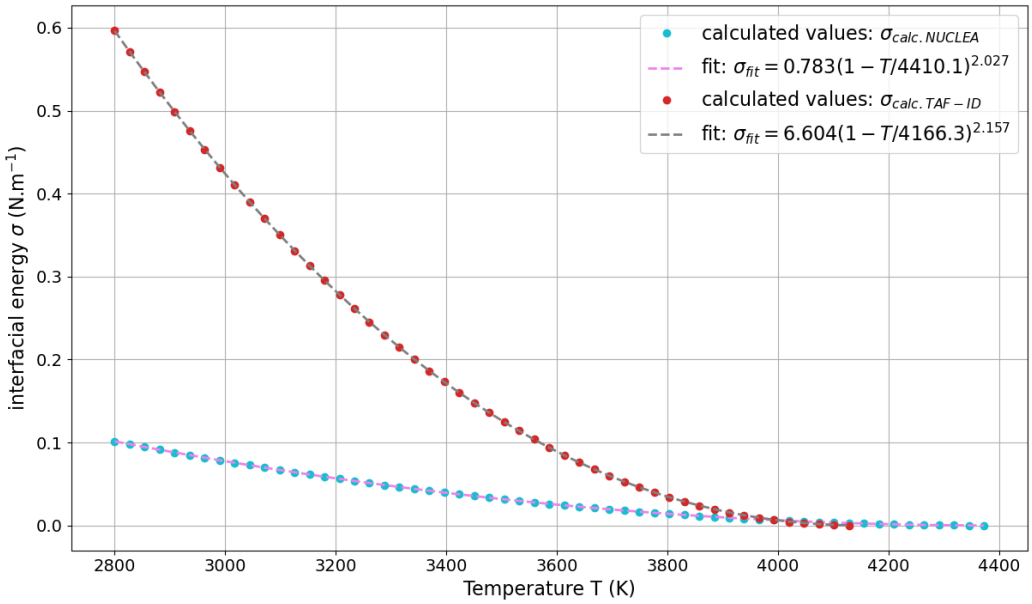

Figure 2: The interfacial energy calculated with the modified code using the NUCLEA and TAF-ID database and plotted against temperature. The dash line is the temperature dependence of the liquid/liquid interfacial tension is plotted using the power law [41].

Which value of ϑ satisfies a given system can be decided only by comparison with experiment. Besides, the experimental data are required for estimation of the constant σ_0. Since measurements of the interfacial tension are not always possible, a theoretical method, which yields correct values of the interfacial tension (at least at the monotectic temperature), is needed. Also, the calculated interfacial energies tend to approach zero at T_C, which is about 4410 K for NUCLEA and 4460 K for TAF-ID databases. At this temperature, also known as the consolute point, the two liquid bulk phases dissolve into a single liquid phase. At T_C, the liquid immiscibility disappears and the calculated interfacial energy is zero. This trend is can be observed in Figure 2 and is also depicted as the monotectic dome in Figure 3.

Critical point exponent for liquid/liquid interfacial tension has been estimated on the basis of experimental data extensively for nonmetallic mixtures. To our knowledge, interfacial tension in liquid metallic systems with a miscibility gap has been measured in a wide temperature interval just in a few studies and the values of critical point exponent established are rather scattered. For some systems, the in-accuracy of the fit or the higher exponent values is attributed to measurements in the miscibility range [45]–[49]. In the work of Hayer *et al.* [46], a comparison of the temperature dependencies of the interfacial tension in the Al-Bi, Al-In and Al-Pb systems determined experimentally with the theoretical predictions are compared. It was deduced that calculated values are approximately 1.5 times less than those measured experimentally. Another point to note is that the theoretical ϑ value ascribed in the renormalization group theory does not deal with the inhearent chemical nature of the systems considered. Therefore, the values for metallic oxide systems could be different just as the case for Al-Si systems [45] despite being the monotectic case. In the present time, the authors have no knowledge of any such studies available in the literature for metallic-oxide systems.

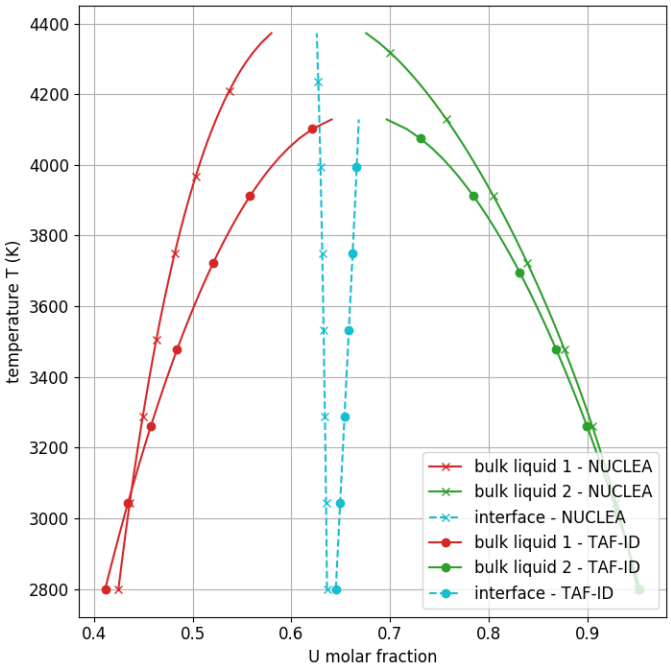

Figure 3: The amount of U in the bulk liquid phase 1 (red) and in the bulk liquid phase 2 (green) and the interfacial U composition (in blue) calculated using the NUCLEA and TAF-ID databases plotted against temperature.

The variation of the molar fraction of 'U' (Figure 3) in the interface is different in NUCLEA and TAF-ID database. In NUCLEA, the mole fraction of U decreases with an increase in temperature and the trend is quite the opposite for TAF-ID. In both the cases, this trend can be consistent as there is a greater solubility of the phases at higher temperatures and the immiscible region begins to converge as we approach the consolute temperature. At T_C, the phases are no longer immiscible and there is no interface formed ($\sigma_{Tc} = 0$) and the bulk phases can no longer be distinguished.

Figure 4 shows the variation of interfacial energy with interface mole fraction 'U' calculated with the NUCLEA and TAF-ID database. Here too, the same contrasting trend can be observed with the values determined for both the databases.

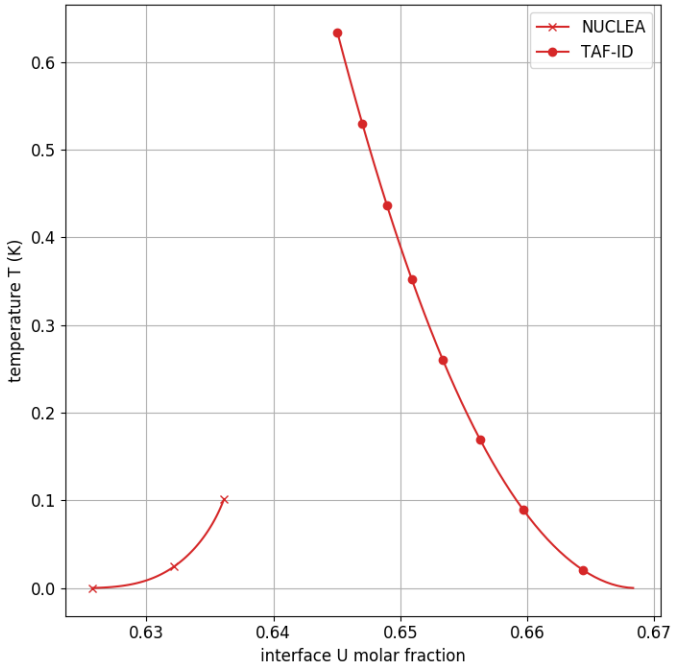

Figure 4: The interfacial energy plotted against interfacial U composition to highlight the variation.

Besides these trends, one can note that the interfacial energy values for TAF-ID seem very high in the temperature range. For the sake of comparison, at room temperature, mercury exhibits the largest surface tension values with about 0.42 $N.m^{-1}$ for Hg-water and 0.49 $N.m^{-1}$ for Hg-air[50].

Girifalco's model [14] allows the evaluation of the interfacial tension σ between domain α and β from the respective surface tension data $\sigma_{\alpha/G}$ and $\sigma_{\beta/G}$ associated with an α / gas and β / gas interface:

$$\sigma = \sigma_{\alpha/G} + \sigma_{\beta/G} - 2\phi\sqrt{(\sigma_{\alpha/G} * \sigma_{\beta/G})} \quad (Eq.8)$$

$$\phi = \frac{4(V_{m,\alpha})^{1/3}(V_{m,\beta})^{1/3}}{\left(4(V_{m,\alpha})^{1/3} + (V_{m,\beta})^{1/3}\right)^2} \quad (Eq.9)$$

where, ϕ is the interfacial interaction parameter that without further information for the U-O system, is expressed from the molar volumes $V_{m,\alpha}$ and $V_{m,\beta}$ (of the α and β phases, respectively) under hard sphere assumption. This model has been the subject of comparison with experimental measurements of interfacial tensions for interfaces between molten steel and slag [51], and for interfaces between organic liquids [52]: the results show good agreement with experimental data.

Such a formula can be used to evaluate an order of magnitude of the interfacial energy in the U-O system considering the limiting case of a UO_2/U interface [2]. Indeed, surface tension data are available in the literature for UO_2/gas and U/gas interfaces [53]. The surface tensions of the oxidic (UO_2/gas) and metallic phase (U/gas) individually are given as [54]:

$$\sigma_{UO_2/G} = 0.513 - 0.19 \cdot 10^{-3}(T - 3120) \pm 17\% \qquad 3120 \leq T \leq 4200K$$

$$\sigma_{U/G} = 2.127 - 0.3365 \cdot 10^{-3}T \pm 10\% \qquad 1405 \leq T \leq 2100K$$

The parameter ϕ in equation 9 is determined from the partial molar volumes of U and O calculated from the NUCLEA and TAF-ID databases using the modified openIEC code. With this input, the interfacial energy obtained at 3200 K (considering that $\sigma_{U/G}$ can be extrapolated at this temperature) are $\sigma_{TAF-ID-Girifalco} = 0.1211\ N.m^{-1}$ and $\sigma_{NUCLEA-Girifalco} = 0.1251\ N.m^{-1}$ respectively. It could also be mentioned that, under a constant molar volume hypothesis ($V_{m,\alpha} = V_{m,\beta}$), the value of the σ interfacial tension at 3200 K is $0.10\ N.m^{-1}$ which is comparable to both previous values.

Such values can be compared with the interfacial energy calculated at 3200 K using the Butler approach developed during this work: $0.2780\ N.m^{-1}$and $0.05629\ N.m^{-1}$ for TAF-ID and NUCLEA database respectively. Both σ values are different from the values obtained by the Girifalco's model and no further conclusions can be drawn at this point.

To better understand the difference between TAF-ID and NUCLEA results, a comparison of the molar volume and chemical potential parameters is presented.

3.1.2 Sensitivity to molar volume and chemical potentials

The interfacial energy calculated using the thermodynamic approach depends strongly on the chemical potential and the molar volume of the phases forming the interface. Since two different databases are used to evaluate the interfacial energy, the impact of the database on these two parameters will be studied to further analyze the differences.

For a coherent liquid/liquid interface, as discussed earlier, the molar volume is calculated based on a second-order finite difference formula. U and O partial molar volumes evolution as a function of the uranium element fraction for the liquid phase is depicted in Figure 5 using both the NUCLEA and TAF-ID databases for T=2800 K. It can be seen that in the range of interest for the interfacial composition, the partial molar volumes are fairly constant with NUCLEA but exhibit larger variations with TAF-ID.

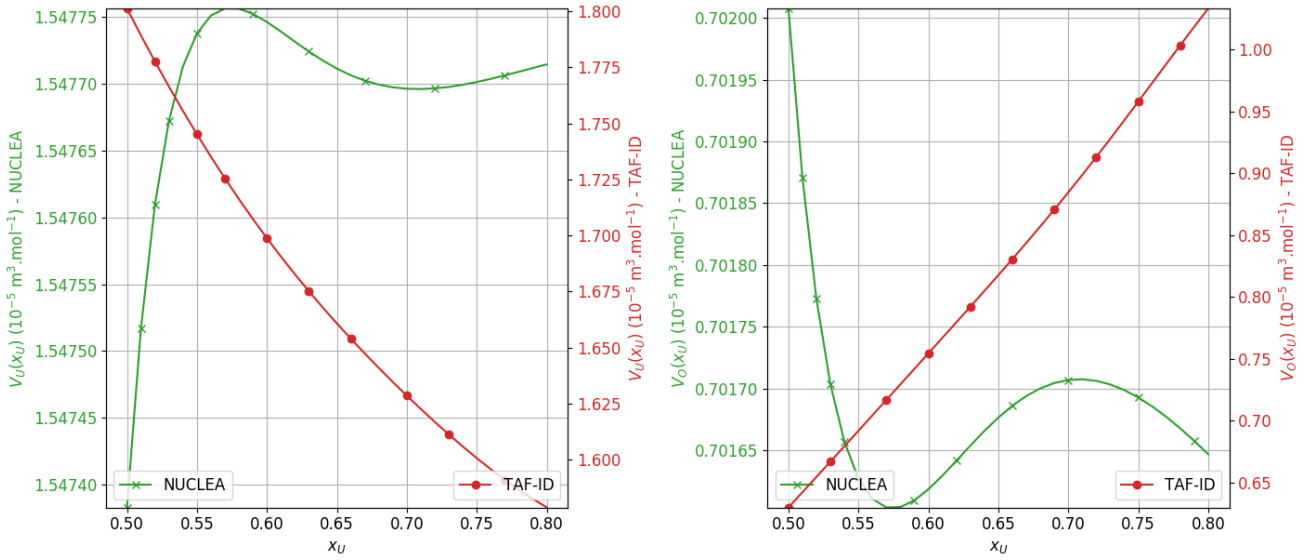

Figure 5: Partial molar volumes for Uranium (left) and Oxygen (right) vs Uranium element fraction for the liquid phase calculated using the NUCLEA and TAF-ID databases (T=2800K).

A sensitivity analysis can be performed at this stage to see the impact of this difference in partial molar volumes on the interfacial energy calculations. For this, interfacial energy is calculated with NUCLEA with full convergence on the partial molar volumes which depend on the interfacial composition. In a second calculation, the partial molar volumes calculated in the previous step (using NUCLEA) are imposed as constant and the interfacial energy is calculated with the TAF-ID database. This calculation leads to the conclusion that the impact of the database on the partial molar volume evaluation is limited; indeed, the fitted values obtained with this approach obey the following law

$$\sigma_{fit} = 7.001\left(1 - \frac{T}{4160.3}\right)^{2.149}$$

that can be compared with the fit associated with TAF-ID in Figure 4:

$$\sigma_{fit} = 6.604\left(1 - \frac{T}{4166.3}\right)^{2.157}$$

Another difference that can be attributed as a consequence of performing the calculation with two databases comes from the chemical potential of the components. To better understand this effect, the chemical potentials are plotted against composition in Figure 6 at T=2800 K. It can be seen that the chemical potentials of the components are vastly different depending on the database even if equilibrium values are fairly consistent. One can conclude that the chemical potential will impact the interfacial energy determined from the databases.

The reason for this difference can be attributed to the lack of experimental data for the U-O-Zr-Fe system and its sub-systems (with the exception of Fe-O) at high temperature. The NUCLEA and TAF-ID databases are based on a fitting procedure to fit the experimental data to obtain the phase diagrams. The phase diagram information is available for lower temperatures in some cases, but the thermodynamic information of the liquid phases and the oxide compounds are largely limited. Without thermodynamic data for the liquid, one can obtain several solutions for the Gibbs energy to obtain the same phase diagram which clearly depends on the degree of freedom of the model chosen to fit the data (associate for NUCLEA of ionic sublattice for the TAF-ID databases). Obtaining additional experimental data is the only way to address this issue.

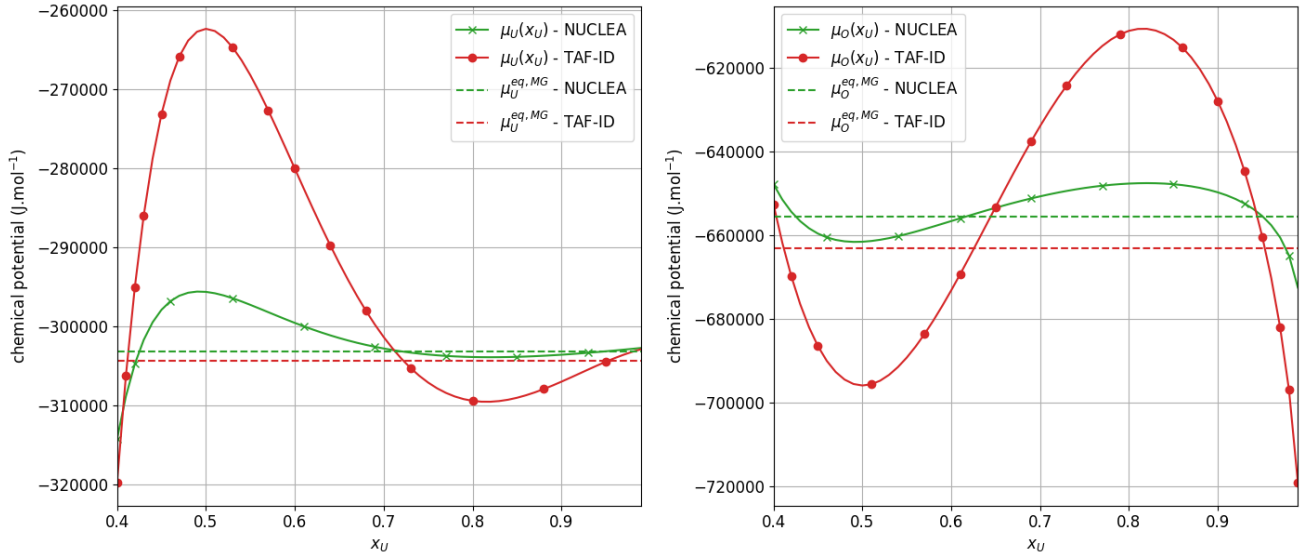

Figure 6: Chemical potential vs. element composition of the liquid phase of the U-O system is calculated using the NUCLEA and TAF-ID databases (T=2800K). In addition, the equilibrium values in the miscibility gap are plotted in dashed lines. We can see the significant amplitude variation for the chemical potentials determined from the two methods even if equilibrium values are rather close.

Moreover, because a miscibility gap is determined by the curvature of the Gibbs energy surface, small changes in the Gibbs energy could lead to possible (and large) modifications in the shape and the extent of the miscibility gap. For example, regarding the miscibility gap in the U-O system, the degree of freedom is large for the liquid and additional data is required to fit many parameters. But, in the state-of-art for this system, the only tie line that has been measured at a given temperature shows that the miscibility gap on the oxygen side is different for NUCLEA and TAF-ID as they treat the experimental data differently. With respect to the pure thermodynamic quantities, the only information available were heat capacity and measure enthalpy of fusion for stoichiometric UO_2 [55].

The heat capacity of UO_2 as a function temperature is shown in Figure 7 that exhibits a rather unusual trend at higher temperatures. For the sake of comparison, the heat capacity of UO_2 is computed with NUCLEA and TAF-ID over a large temperature range and the results are shown in Figure 8. Here, in the CALPHAD assessment for the liquid phase, heat capacity is considered as almost constant for NUCLEA, but a different trend for TAF-ID, which is fairly consistent to experimental data shown in Figure 7. The variation contrasts can be attributed to the data considered in developing the database and in the modeling procedure.

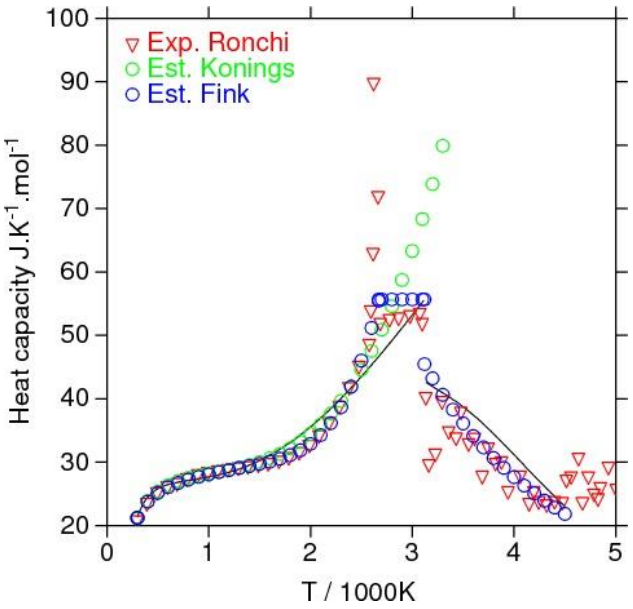

Figure 7: Heat capacity of UO2 plotted a function of temperature using the data available in the literature [55].

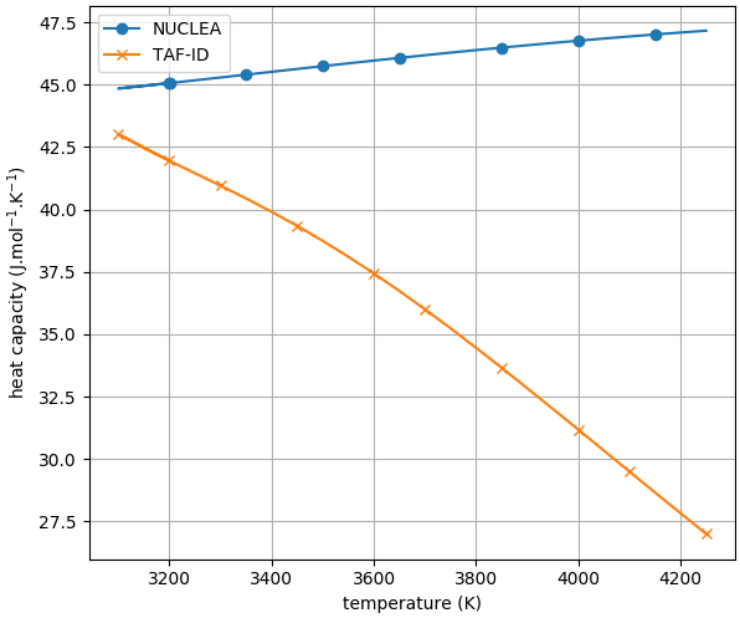

Figure 8: Heat capacity of UO2 plotted as a function of temperature using the NUCLEA and TAF-ID databases.

3.2 U-O-Zr-Fe quaternary system

The modified code was extended to the U-O-Zr-Fe quaternary system and the interfacial energies were calculated over a range of compositions in the miscibility region. In this section, the results for one such

composition and the observations on the versatility of the new code for this complex system will be discussed.

3.2.1 Towards a more robust numerical solution of the Butler equation

So far, for all U-O binary calculations, the non-linear system given by Eq. 3 has been solved with the standard procedure used in openIEC based on the Nelder-Mead algorithm. Considering the interface composition as initial guess, the average between both phases compositions at equilibrium was found to be a simple and practical way to ensure proper convergence of such an algorithm without further tuning.

When considering the solution to the Butler equation for the *N*-ary case (*N*>2), such a simple approach is no longer effective and non-convergence or false-convergence can be observed. Indeed, the associated optimization problem is not as trivial as it may look. First of all, finding an "optimal" starting point for the interfacial composition cannot easily be set in the general case. In particular, contrarily to the binary case, the interfacial composition in the *N*-ary case (*N*>2) can be out of the range associated with the bulk equilibrium compositions for some components. The choice of this starting point is very important in order to avoid the optimization algorithm to end-up with the incorrect "trivial" solution of Butler equations: $\forall i \in [1, N-1], x_{i,\zeta} = x_i^{\alpha}\ or\ x_i^{\beta}$ and $\sigma = 0$. Then, with the Nelder-Mead algorithm, we cannot enforce that the composition remains in the feasible domain $\{\forall \mathrm{i} \in [1, N]\ 0 < x_{i,\zeta} < 1$ such that $\sum_{j=1}^{N} x_{j,\zeta} = 1\}$.

To solve these issues, an alternative method known as the trust-region constrained method has been used. With such a method, it is possible to impose both linear and non-linear constraints to the minimization algorithm. First, linear constraints are written as:

$$\begin{bmatrix} 0 \\ 0 \\ 0 \\ 0 \end{bmatrix} \leq \begin{bmatrix} 1 & 0 & 0 \\ 0 & 1 & 0 \\ 0 & 0 & 1 \\ 1 & 1 & 1 \end{bmatrix} \begin{bmatrix} x_{1,\zeta} \\ x_{2,\zeta} \\ x_{3,\zeta} \end{bmatrix} \leq \begin{bmatrix} 1 \\ 1 \\ 1 \\ 1 \end{bmatrix}$$

in order to ensure that the optimization algorithm only takes valid composition points. Then, to avoid that the trivial solution $\sigma = 0$ is found, spheres of exclusion around the bulk compositions are defined through non-linear constraints as,

$$\begin{bmatrix} r_\varepsilon \\ r_\varepsilon \end{bmatrix} \leq \begin{bmatrix} \sqrt{\sum_{i=1}^{N-1} \left(x_{i,\zeta} - x_i^\alpha\right)^2} \\ \sqrt{\sum_{i=1}^{N-1} \left(x_{i,\zeta} - x_i^\beta\right)^2} \end{bmatrix}$$

with, in practice, r_ε the sphere radius, set to 10^{-6}.

The implementation of the optimization algorithm as provided by the scipy module has been used.

3.2.2 Numerical results

First of all, for a given global composition in the liquid miscibility gap defined by composition $x_U = 0.18832, x_{Zr} = 0.15693, x_{Fe} = 0.12118$, the interfacial energy has been evaluated over the 2900-5100 K temperature range with NUCLEA database with full convergence on the partial molar volumes which depend on the interfacial composition. This global composition corresponds to a U/Zr molar ratio $R_{U/Zr}$ of 1.2 (typical of a Pressurized Water Reactor core inventory), a Zr oxidation degree C_{Zr} of 0.5 (this value typical varies between 0.3 and 1.0 depending on the how fast is the accident transient is) and a mass ratio between Fe and (U,Zr,O) (denoted x_{steel}) of 0.1. As in the U-O case, the analysis was conducted on a large temperature range (above the temperature at which a gas phase is predicted e.g. with NUCLEA at about 3260K at 1bar) in order to study the model behavior and check its consistency.

The results are depicted in terms of interfacial energy as a function temperature and interfacial composition as a function of interfacial energy in Figure 9. As expected, the interfacial energy is found decreasing with temperature and it follows a 'power law' as in the binary U-O case in Figure 2. However, we see that ϑ is lower than the binary case, but still significantly higher than the theoretical value 1.26. When considering the evolution of the interfacial energy as a function of the interfacial composition, it

is interesting to note that it is monotonously increasing with U and Zr molar fraction and decreases with the Fe molar fraction.

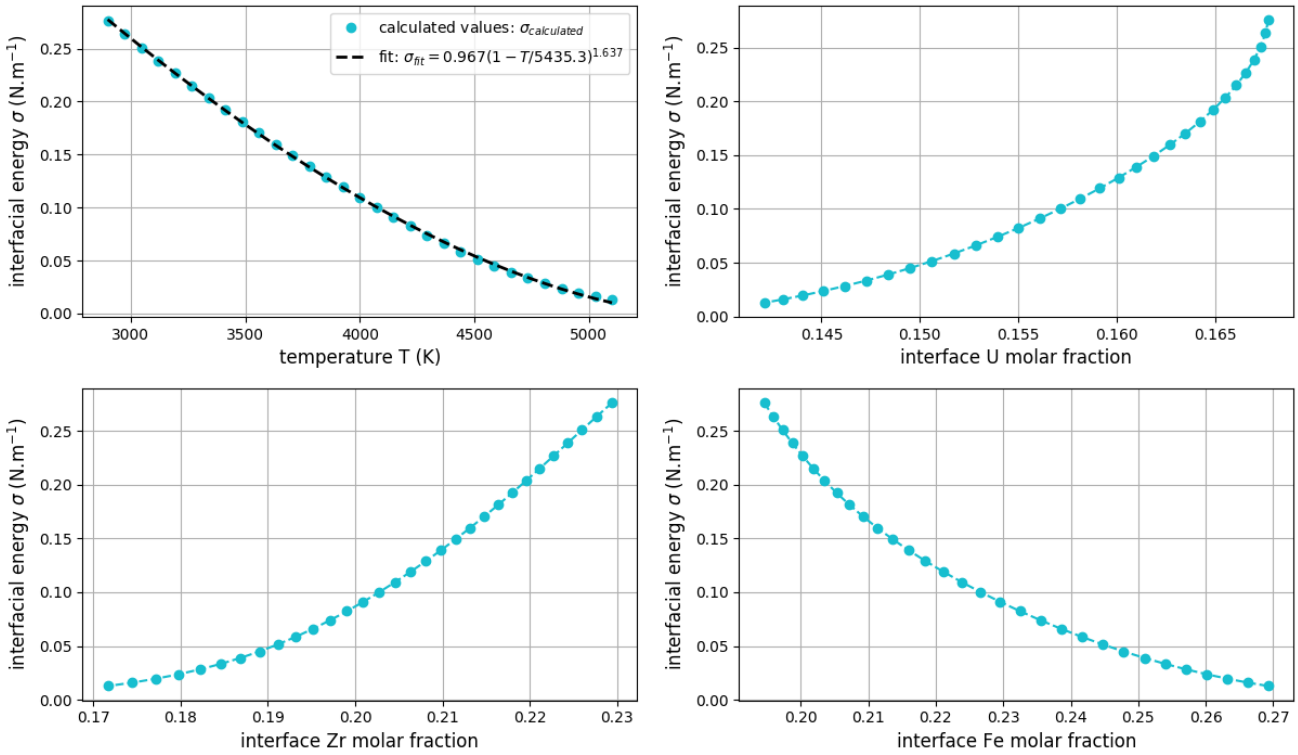

Figure 9: From top left, clockwise - Interfacial energy as a function of temperature, U, Zr or Fe molar fraction in the interface calculated using the NUCLEA database in the 2900-5100 K temperature range for an average composition $x_U = 0.18832, x_{Zr} = 0.15693, x_{Fe} = 0.12118$.

Then, in order to illustrate the robustness of our solution of the Butler equations based on the trust-region constrained method described in the previous section, for fixed values of the temperature T=3000 K and $R_{U/Zr}$=1.2, the interfacial energy was evaluated over the compositional domain of interest for in-vessel corium behavior by varying C_{Zr} in $\{0.3, 0.5, 0.7, 0.9\}$ and x_{steel} in $\{0.1, 0.2, 0.3, 0.4, 0.5, 0.6, 0.7, 0.8, 0.9, 1.0\}$. Both NUCLEA and TAF-ID databases were used and, in both cases, interfacial energies were evaluated with full convergence on the partial molar volumes that depend on the interfacial composition.

The results in terms of interfacial energy and composition (both of the interface and the bulk phases) are depicted in Figure 10 and Figure 11 for NUCLEA and TAF-ID respectively. In all cases, the interfacial energy is found monotonously increasing when x_{steel} increases and the lower C_{Zr} is, the larger the variation amplitude of the interface energy overall the complete x_{steel} range is. This trend is consistent with the fact that the bulk phase compositions are most sensitive to C_{Zr} or x_{steel} parameters in the compositional range where C_{Zr} and x_{steel} have small values. As observed before on the U-O system, NUCLEA and TAF-ID databases result significantly differ with an interfacial energy about three times higher when evaluated with TAF-ID. As commented earlier, the reason for this difference can be attributed to the high sensitivity of the Butler equation to the extrapolation of the chemical potentials out of global equilibrium conditions where NUCLEA and TAF-ID databases significantly differ because of the lack of experimental data for the U-O-Zr-Fe system.

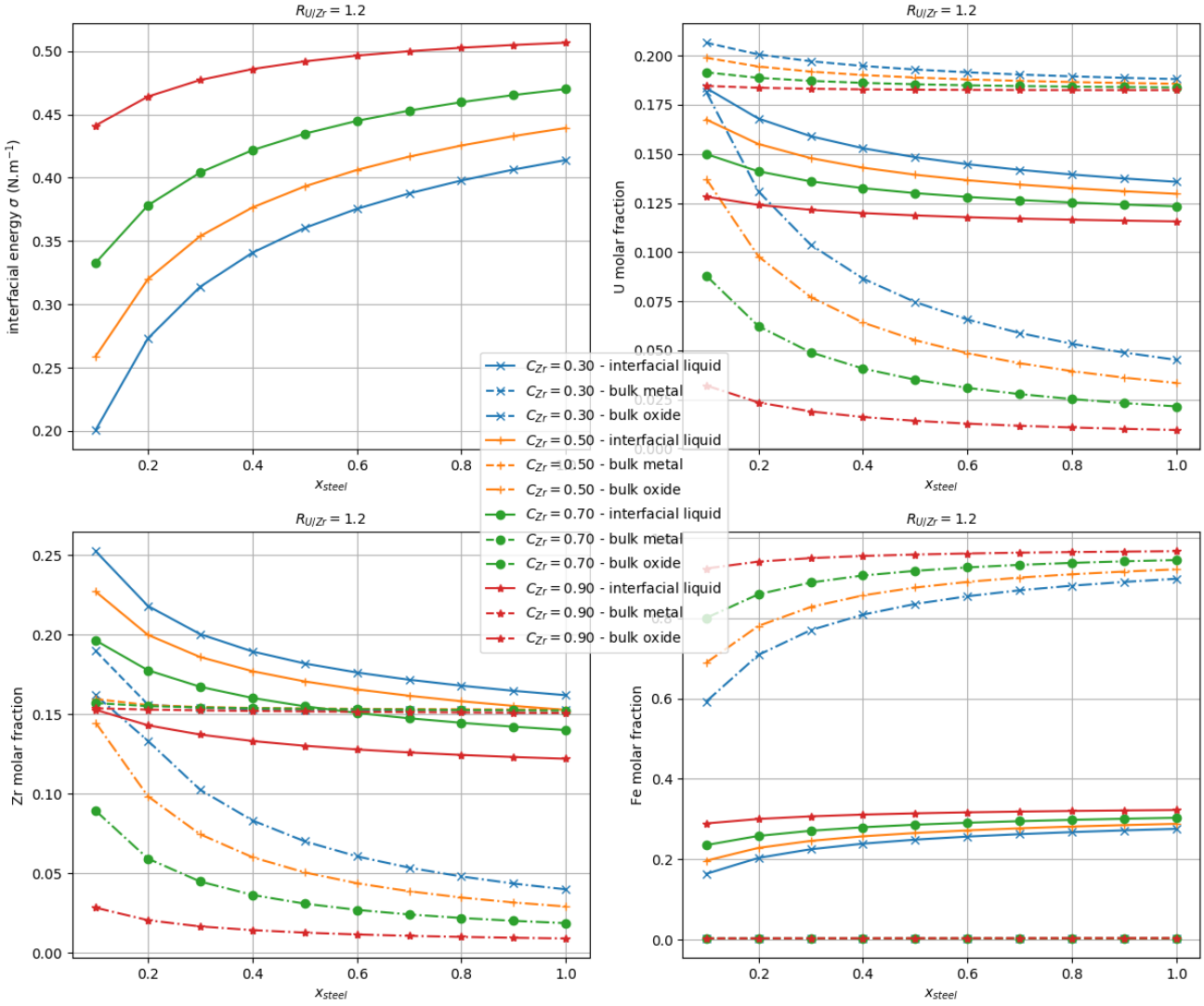

Figure 10: From top left, clockwise - Interfacial energy, U, Zr and Fe molar fractions in the interface and the bulk phases calculated using the NUCLEA database plotted as a variation of x_{steel} for various C_{Zr} and $R_{U/Zr}$=1.2.

When looking at the evolution of the interfacial composition as a function of x_{steel}, it is interesting to compare it with the two bulk phase compositions as proposed in Figure 10 and Figure 11. Indeed, as discussed in section 3.2.1, the interfacial composition in the *N*-ary case (*N*>2) can be, for some component, out of the range associated with the bulk equilibrium compositions. This can be clearly observed for the Zr component in all cases for the TAF-ID results and for low enough values of C_{Zr} or x_{steel} parameters with NUCLEA database. This trend can be related to the well-known surface adsorption in a *N*-ary (*N*>2) system that can lead to non-monotonic composition profile when over a diffuse interface separating two phases under equilibrium. In this case, the observed trend of a Zr-

enrichment of the interfacial composition is consistent with the composition profiles obtained by numerical simulations with a Cahn-Hilliard model in [54] where the U-O-Zr-Fe Gibbs energy description was extracted from an older version of the NUCLEA database.

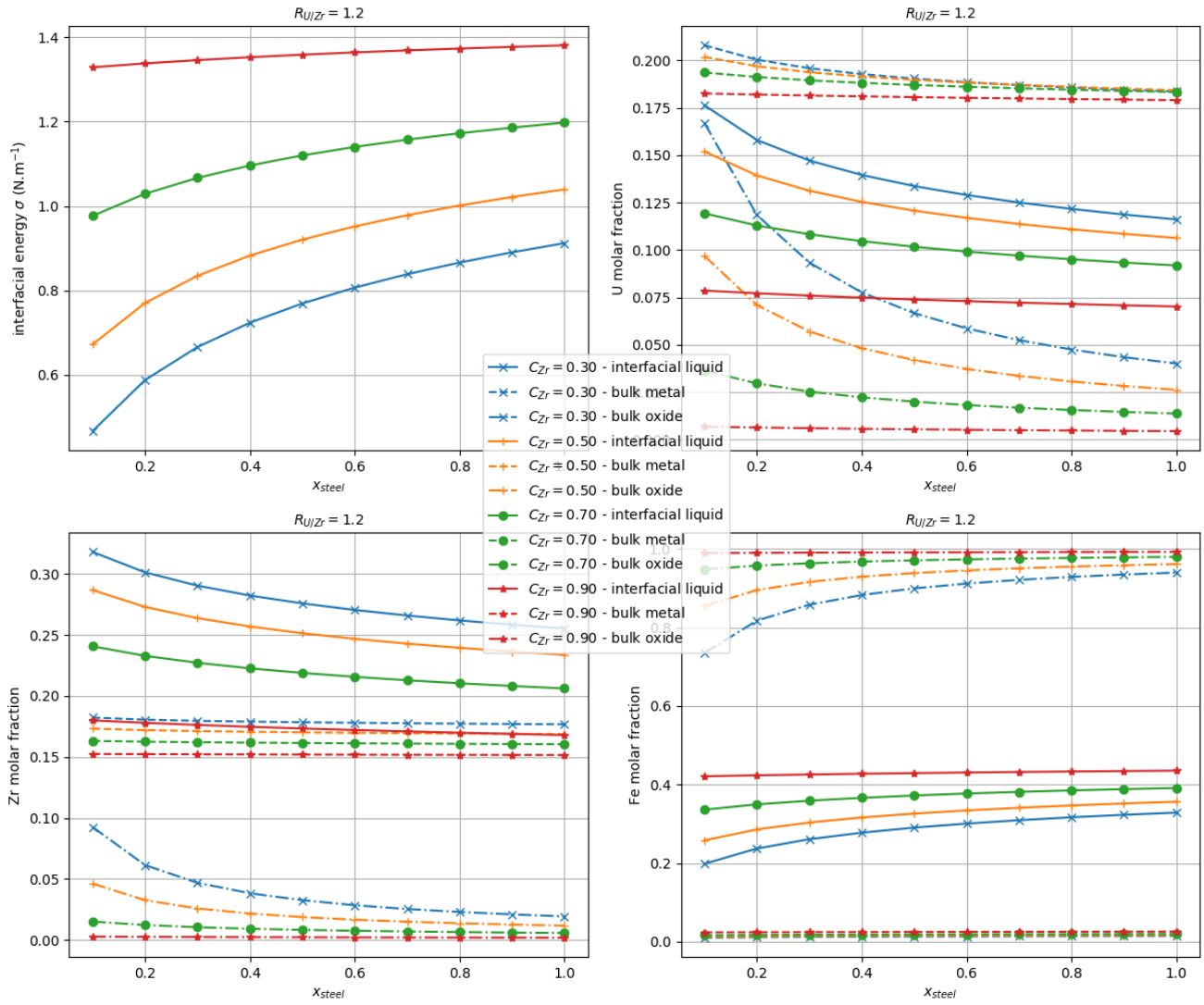

Figure 11: From top left, clockwise - Interfacial energy, U, Zr and Fe molar fractions in the interface and the bulk phases calculated using the TAF-ID database plotted as a variation of x_{steel} for various C_{Zr} and $R_{U/Zr}$=1.2.

4 CONCLUSIONS AND PERSPECTIVES

The article explores the possibility of evaluating the interfacial energies for corium systems through a thermodynamic approach. The thermodynamic connection was established by the Butler equation

mainly from the renovated Butler equation extended to coherent interfaces in the studies of Kaptay [3]. The openIEC code using pyCalphad [4] was modified accordingly with the tools developed at CEA to enhance proper treatment of metastable phases in miscibility gap and address drawbacks in partial molar volume computation methodology (first order volume derivatives approximated by on a second-order finite difference formula) and interfaced with OpenCalphad.

With the numerical code in place, the study opens new frontiers to evaluate the interfacial energies by thermodynamic approaches with existing thermodynamic tools. The code was tested for the U-O binary system and was able compute the interfacial energies for the liquid/liquid interface over a large temperature range (up to the consolute point) using both NUCLEA and TAF-ID databases. Parametric studies were carried on the U-O system using the two databases. The subsequent results were analyzed and the discrepancies between both databases were attributed to the lack experimental information, especially the thermodynamic information at the very high temperatures. With this successful step, the code was applied U-O-Zr-Fe system and results were obtained over a large range of compositions (covering the domain of interest for corium modelling) in order to highlight the robustness of the numerical procedure developed for the solution of the Butler equation.

At this stage of development of the NUCLEA and TAF-ID databases, because of the limited experimental data for the liquid phase, extrapolation of the liquid chemical potentials far from equilibrium is very uncertain. Accordingly, the results obtained in this paper for the interfacial energies in the liquid miscibility gap exhibit important differences between both databases and should not be considered as quantitatively reliable. However, as discussed, these results exhibit qualitatively consistent trends that have been analyzed and give confidence in the methodology itself. Hence, future improvement of the liquid phase modelling in these databases thanks to new calorimetry data could make it possible to obtain quantitative data for liquid/liquid interfacial energies through the approach developed in the present work.

In the near future, this approach will be used for calculating interfacial energies for nuclear glasses starting with the ternary system (SiO_2, Na_2O, MoO_3) in order to provide adequate parameterization of demixing models. Moreover, the code could be extended to accommodate non-coherent interfaces, for example, the solid/liquid interfaces which are perquisite to modeling the Marangoni convection during cooling and solidification. With no experimental information for the corium systems in place in the far future, the authors also suggest integration of surface tension data (through the same Butler equation approach) in the assimilation process that is used to create the thermodynamic databases by calibration of the thermodynamic parameters.

ACKNOWLEDGEMENTS

This work was funded in the frame of the TICOV project ("vers une approche Thermodynamique pour la modélisation des énergies Interfaciales relatives au COrium et aux Verres nucléaires") funded by the "Bottom Up" initiative of CEA "Programmes Exploratoire et Transversaux de Compétences". This project was constructed with the help of Sophie Schuller (CEA, DES, ISEC, DE2D), Christine Guéneau (CEA, DES, ISAS, DPC) and Jules Delacroix (CEA, DES, IRESNE, DTN) that the authors would like to thank for their valuable inputs and suggestions on taking the project forward.

REFERENCES

[1] V. Tiwari, "A Consistent Approach for Coupling Lumped-Parameter and Phase-Field Models for In-vessel Corium to Thermodynamic Databases," Interfaces-Approches Interdisciplinaires: Fondements, Applications et Innovation, Université Paris-Saclay, 2019.

[2] C. Cardon, R. Le Tellier, and M. Plapp, "CALPHAD : Computer Coupling of Phase Diagrams and Modelling of liquid phase segregation in the Uranium – Oxygen binary system," *Calphad*, vol. 52, pp. 47–56, 2016, doi: 10.1016/j.calphad.2015.10.005.

[3] G. Kaptay, "On the interfacial energy of coherent interfaces," *Acta Mater.*, vol. 60, no. 19, pp.

6804–6813, 2012, doi: 10.1016/j.actamat.2012.09.002.

[4] S. Yang, J. Zhong, J. Wang, L. Zhang, and G. Kaptay, “OpenIEC: an open-source code for interfacial energy calculation in alloys,” *J. Mater. Sci.*, vol. 54, no. 14, pp. 10297–10311, 2019, doi: 10.1007/s10853-019-03639-w.

[5] M. Kurata, M. Osaka, D. Jacquemain, M. Barrachin and T. Haste, “Advances in fuel chemistry during a severe accident: Update after Fukushima Daiichi Nuclear Power Station (FDNPS) accident,” *Adv. Nucl. Fuel Chem.*, pp. 555–625, 2020, doi: https://doi.org/10.1016/B978-0-08-102571-0.00015-X.

[6] A. Cartalade, A. Younsi, and M. Plapp, “Lattice Boltzmann simulations of 3D crystal growth : Numerical schemes for a phase-field model with anti-trapping current Lattice Boltzmann simulations of 3D crystal growth : Numerical schemes for a phase-field model with anti-trapping current,” *Comput. Math. with Appl.*, vol. 71, no. 9, pp. 1784–1798, 2016, doi: 10.1016/j.camwa.2016.02.029.

[7] A. Cartalade, A. Younsi, É. Régnier, and S. Schuller, “Simulations of Phase-field Models for Crystal Growth and Phase Separation,” *Procedia Mater. Sci.*, vol. 7, no. 0, pp. 72–78, 2014, doi: 10.1016/j.mspro.2014.10.010.

[8] R. Zanella, R. Le Tellier, M. Plapp, G. Tegze and H. Henry, “Numerical Simulation of Droplet Formation by Rayleigh Taylor Instability in Multiphase Corium.” *Nucl. Eng. Des.*, vol. 379, 111177, 2021.

[9] H. L. Lukas, S. G. Fries, and B. Sundman, *Computational Thermodynamics ; The Calphad method*. Cambridge University Press, The edinburgh Building, Cambridge CB2 8RU, UK, 2007.

[10] S. Gossé, C. Guéneau, S. Bordier, S. Schuller, A. Laplace, and J. Rogez, “A Thermodynamic Approach to Predict the Metallic and Oxide Phases Precipitations in Nuclear Waste Glass Melts A Thermodynamic Approach to predict the Metallic and Oxide Phases Precipitations in Nuclear Waste Glass Melts,” *Procedia Mater. Sci.*, vol. 7, no. January 2015, pp. 79–86, 2014, doi: 10.1016/j.mspro.2014.10.011.

[11] V. Bouyer, N. Cassiaut-Louis, P. Fouquart, and P. Piluso, “Plinius prototypic corium experimental platform: Major results and future works,” *Int. Top. Meet. Nucl. React. Therm. Hydraul. 2015, NURETH 2015*, vol. 7, pp. 5327–5340, 2015.

[12] P. Piluso, J. Monerris, C. Journeau, and G. Cognet, “Viscosity Measurements of Ceramic Oxides by Aerodynamic Levitation 1,” *Int. J. of Thermophysics*, vol. 23, no. 5, pp. 1229–1240, 2002.

[13] D. Manara, A. Seibert, T. Gouder O. Beneš, L. Martel, J.-Y. Colle, J.-C. Griveau, O. Walter, A. Cambriani, O. Dieste Blanco, D. Staicu, T. Wiss and J.-F. Vigier, “Chapter-2 Experimental methods,” in *Advances in Nuclear Fuel Chemistry*, Elsevier, 2020, pp. 89–158.

[14] L. A. Girifalco and R. J. Good, “A theory for the estimation of surface and interfacial energies. I. Derivation and application to interfacial tension,” *J. Phys. Chem.*, vol. 61, no. 7, pp. 904–909, 1957, doi: 10.1021/j150553a013.

[15] J. Korozs and G. Kaptay, “Derivation of the Butler equation from the requirement of the minimum Gibbs energy of a solution phase, taking into account its surface area,” *Colloids Surfaces A Physicochem. Eng. Asp.*, 2017, doi: 10.1016/j.colsurfa.2017.09.010.

[16] M. Barrachin, “Corium Experimental Thermodynamics: A Review and Some Perspectives,” *Thermo*, vol. 1, no. 2, pp. 179–204, 2021, doi: 10.3390/thermo1020013.

[17] E. Fischer, “NUCLEA Thermodynamic Database for Corium, and Mephista Thermodynamic Database for Fuel Applications,” 2021.

[18] C. Guéneau, N. Dupin, L. Kjellqvist, E. Geiger, M. Kurata, S. Gossé, E. Corcoran, A. Quaini, R. Hania, A.L. Smith, M.H.A. Piro, T. Besmann, P.E.A. Turchi, J.C. Dumas, M.J. Welland, T. Ogata, B.O. Lee, J.R. Kennedy, C. Adkins, M. Bankhead and D. Costa, “TAF-ID: An international thermodynamic database for nuclear fuels applications,” *Calphad*, vol. 72, p. 102212, Mar. 2021, doi: 10.1016/j.calphad.2020.102212.

[19] J. W. Gibbs, “On the Equilibrium of Heterogeneous Substances,” *Trans. Conn. Acad. Arts Sci.*, vol. 3, p. 108–248 and 343–524.

[20] G. Kaptay, “Partial surface tension of components of a solution,” *Langmuir*, vol. 31, no. 21, pp.

5796–5804, 2015, doi: 10.1021/acs.langmuir.5b00217.

[21] M. Soledade, C. S. Santos, J. Carlos, and R. Reis, “Partial molar surface areas in liquid mixtures . Theory and evaluation in aqueous ethanol,” *J. Mol. Liq.*, vol. 273, pp. 525–535, 2019, doi: 10.1016/j.molliq.2018.10.057.

[22] B. Sundman , Ursula R. Kattner, Christophe Sigli, Matthias Stratmann, Romain Le Tellier, Mauro Palumbo and Suzana G. Fries, “The OpenCalphad Thermodynamic Software Interface,” *Comput. Mater. Sci.*, vol. 125, pp. 188–196, 2016, doi: 10.1016/j.commatsci.2016.08.045.

[23] R. Pajarre, P. Koukkari, T. Tanaka, and J. Lee, “Computing surface tensions of binary and ternary alloy systems with the Gibbsian method,” *Calphad Comput. Coupling Phase Diagrams Thermochem.*, vol. 30, no. 2, pp. 196–200, 2006, doi: 10.1016/j.calphad.2005.08.003.

[24] R. Otis and Z.-K. Liu, “pycalphad: CALPHAD-based Computational Thermodynamics in Python,” *J. Open Res. Softw.*, vol. 5, pp. 1–11, 2017, doi: 10.5334/jors.140.

[25] J. R. Kermode, “f90wrap: An automated tool for constructing deep Python interfaces to modern Fortran codes,” *J. Phys. Condens. Matter*, vol. 32, no. 30, 2020, doi: 10.1088/1361-648X/ab82d2.

[26] R. Kermode , J, A. Bartok Partay, N. Bernstein, and G. Csanyi, “Libatoms, Quip and Gap,” *URL: http://libatoms. github.io. .*

[27] S. J. Clark, M. D. Segall, C. J. Pickard, P. J. Hasnip, M. I. J. Probert, K. Refson and M. C. Payne, “First Principles Methods Using CASTEP,” *Zeitschrift fur Krist.*, vol. 220, no. 5–6, pp. 567–570, 2005, doi: 10.1524/zkri.220.5.567.65075.

[28] G. Kaptay, “Approximated equations for molar volumes of pure solid fcc metals and their liquids from zero Kelvin to above their melting points at standard pressure,” *J. Mater. Sci.*, vol. 50, no. 2, pp. 678–687, 2014, doi: 10.1007/s10853-014-8627-z.

[29] M. Barrachin and F. Defoort, “Thermophysical Properties of In-vessel Corium : MASCA Programme Related Results,” *OECD Nucl. Energy Agency*, 2018.

[30] B. Cheynet and P. Chaud, “NUCLEA ‘Propriétés Thermodynamiques et Equilibres de Phases

dans les Systèmes d'intérêt Nucléaire,'" *J. Phys. IV Fr.*, vol. 113, pp. 61–64, 2004, doi: 10.1051/jp4:20040014.

[31] S. Bakardjieva , M. Barrachin, S. Bechta, D. Bottomley, L. Brissoneau, B. Cheynet, E. Fischer, C. Journeau, M. Kiselova, L. Mezentseva, P. Piluso and T. Wiss, "Improvement of the European Thermodynamic Database NUCLEA," *Prog. Nucl. Energy*, vol. 52, no. 1, pp. 84–96, Jan. 2010, doi: 10.1016/J.PNUCENE.2009.09.014.

[32] S. Massara and C. Guéneau, "Thermodynamics of advanced fuels - international database project," *NEA News,* vol. 32, no. 1, pp. 24–25, 2014.

[33] P. Y. Chevalier, E. Fischer, and B. Cheynet, "Progress in the thermodynamic modelling of the O-U binary system," *J. Nucl. Mater.*, vol. 303, no. 1, pp. 1–28, 2002, doi: 10.1016/S0022-3115(02)00813-9.

[34] C. Guéneau, V. Dauvois, P. Pérodeaud, C. Gonella, and O. Dugne, "Liquid immiscibility in a (O,U,Zr) model corium," *J. Nucl. Mater.*, vol. 254, no. 2–3, pp. 158–174, Apr. 1998, doi: 10.1016/S0022-3115(98)00002-6.

[35] J. Assal, B. Hallstedt, and L. J. Gauckler, "Thermodynamic Assessment of the Ag-Cu-O System," *J. Phase Equilibria*, vol. 19, no. 4, pp. 351–360, 1998, doi: 10.1016/j.jallcom.2005.06.060.

[36] M. Baichi, C. Chatillon, G. Ducros, and K. Froment, "Thermodynamics of the O-U system: III - Critical assessment of phase diagram data in the U-UO2+x composition range," *J. Nucl. Mater.*, vol. 349, no. 1–2, pp. 57–82, Feb. 2006, doi: 10.1016/j.jnucmat.2005.10.001.

[37] M. Baichi, C. Chatillon, G. Ducros, and K. Froment, "Thermodynamics of the O-U system. IV - Critical assessment of chemical potentials in the U-UO2.01 composition range," *J. Nucl. Mater.*, vol. 349, no. 1–2, pp. 17–56, Feb. 2006, doi: 10.1016/j.jnucmat.2005.09.001.

[38] C. Guéneau, V. Dauvois, P. Pérodeaud, C. Gonella, and O. Dugne, "Liquid immiscibility in a (O,U,Zr) model corium," *J. Nucl. Mater.*, vol. 254, no. 2–3, pp. 158–174, 1998, doi: 10.1016/S0022-3115(98)00002-6.

[39] P. Y. Chevalier, E. Fischer, and B. Cheynet, “Progress in the thermodynamic modelling of the O-U-Zr ternary system,” *Calphad Comput. Coupling Phase Diagrams Thermochem.*, vol. 28, no. 1, pp. 15–40, 2004, doi: 10.1016/j.calphad.2004.03.005.

[40] A. Quaini , C. Guéneau, S. Gossé, N. Dupin, B. Sundman, E. Brackx, R. Domenger, M. Kurata and F. Hodaj, “Contribution to the thermodynamic description of the corium – The U-Zr-O system,” *J. Nucl. Mater.*, vol. 501, pp. 104–131, 2018, doi: 10.1016/j.jnucmat.2018.01.023.

[41] J. Ataiyan and D. Woermann, “Temperature dependence of liquid/liquid and liquid/gas interfacial tensions in binary liquid mixtures with a miscibility gap: Study of the system 2=butoxyethanol/water in the vicinity of its lower critical point,” *Pure annd Appl. Chem.*, vol. 67, no. 6, pp. 889–895, 1995.

[42] J. D. van der Waals, “Thermodynamische Theorie der Kapillarität unter Voraussetzung stetiger Dichteänderung,” *Zeitschrift für Phys. Chemie*, vol. XIII, no. 1, p. 657, 1894, doi: 10.1515/zpch-1894-1338.

[43] J. W. Cahn and J. E. Hilliard, “Free energy of a nonuniform system. I. Interfacial free energy,” *J. Chem. Phys.*, vol. 28, no. 2, pp. 258–267, 1958, doi: 10.1063/1.1744102.

[44] J. S. Rowlinson and M. Widom, *Molecular theory of capillarity*. 1982.

[45] I. Kaban, J. Gröbner, W. Hoyer, and R. Schmid-Fetzer, “Liquid-liquid phase equilibria, density difference, and interfacial tension in the Al-Bi-Si monotectic system,” *J. Mater. Sci.*, vol. 45, no. 8, pp. 2030–2034, 2010, doi: 10.1007/s10853-009-3713-3.

[46] W. Hoyer, I. Kaban, and M. Merkwitz, “Liquid-liquid interfacial tension in immiscible binary Al-based alloys,” *J. Optoelectron. Adv. Mater.*, vol. 5, no. 5, pp. 1069–1073, 2003.

[47] W. Hoyer and I. Kaban, “Demixing Metal Alloys,” vol. 25, no. 5, pp. 452–456, 2006.

[48] I. Kaban and W. Hoyer, “Liquid–liquid interfacial tension in the monotectic alloy (Al34.5Bi65.5)95Si5 (wt.%),” *Int. J. Mat. Res. (formerly Z. Met. 97*, vol. 4, pp. 362–364, 2006.

[49] A.-B.-S. I. Kaban, W. Hoyer, and M. Kehr, “Liquid-Liquid Interfacial Tension in Ternary Monotectic Alloys,” *Int. J. Thermophys.*, vol. 28, no. 2, 2007, doi: 10.1007/s10765-007-0184-

0.

[50] A. W. Adamson and A. P. Gast, *Physical chemistry of surfaces*. 1967.

[51] T. Tanaka and S. Hara, "Application of thermodynamic databases to evaluation of interfacial tension between liquid steels and molten slags," *Zeitschrift fuer Met. Res. Adv. Tech.*, vol. 90, no. 5, pp. 348–354, 1999.

[52] A. Yasumori, G. F. Neilson, and M. C. Weinberg, "Measurement of surface tension of organic liquid pairs," *J. Colloid Interface Sci.*, vol. 155, no. 1, pp. 85–91, Jan. 1993, doi: 10.1006/jcis.1993.1013.

[53] International Atomic Energy Agency, Thermophysical properties of materials for nuclear engineering : a tutorial and collection of data. Vienna: International Atomic Energy Agency, 2008.

[54] C. Cardon, "Modélisation de la diffusion multi-composants dans un bain de corium diphasique oxyde-métal par une méthode d ' interface diffuse," Université Paris-Saclay, prepared at l´école polytechnique, 2017.

[55] C. Guéneau , N. Dupin, B. Sundman, C. Martial, J.-C. Dumas, S. Gossé, S. Chatain, F. De Bruycker, D. Manara and R. J.M. Konings, "Thermodynamic modelling of advanced oxide and carbide nuclear fuels: Description of the U-Pu-O-C systems," *J. Nucl. Mater.*, vol. 419, no. 1–3, pp. 145–167, 2011, doi: 10.1016/j.jnucmat.2011.07.033.